

Coherence-based Underwater Target Detection for Side-Scan Sonar Imagery

J. Derek Tucker

Department of Electrical & Computer Engineering

Adviser: Dr Mahmood R. Azimi-Sadjadi

Department of Electrical & Computer Engineering

Committee Members:

Dr. J. Rocky Luo

Department of Electrical & Computer Engineering

Dr. F. Jay Breidt

Department of Statistics

M.S. Defense - February 27, 2009

This work was supported by the Office of Naval Research, Code 321OE

Outline of Presentation

- ✓ Introduction
 - Background
 - Research Goals and Motivations
- ✓ Sonar Imagery Data Sets
 - Preprocessing Methods
- ✓ Gauss - Gauss Detection
 - Standard One Channel Detector
 - Two Channel Detector
- ✓ Coherence-based Underwater Target Detection
 - Single Sensor Case
 - Dual Disparate Sensor Case
 - Distributed Detection
- ✓ Sample Support of Gauss - Gauss Detection
 - Sample Rich and Sample Poor
 - Kernel Gauss - Gauss Detection
- ✓ Conclusions and Future Work

Problem Statement & Background

Exploit coherence between two or more images generated from disparate (location, frequency, resolution, etc.) sonar systems to perform multi-platform underwater target detection

Complications:

- ✓ Variations in operating and environmental conditions with spatially varying clutter
- ✓ Variations in target shapes, compositions, and orientations
- ✓ Lack of a priori knowledge about the shape and geometry of new non-mine-like objects that may be encountered

Problems / Approaches:

Problem Statement & Background

Exploit coherence between two or more images generated from disparate (location, frequency, resolution, etc.) sonar systems to perform multi-platform underwater target detection

Complications:

- ✓ Variations in operating and environmental conditions with spatially varying clutter
- ✓ Variations in target shapes, compositions, and orientations
- ✓ Lack of a priori knowledge about the shape and geometry of new non-mine-like objects that may be encountered

Problems / Approaches:

- ✓ Single Sensor
 - Limited field of view and targets vary as a function of aspect, grazing angle, and range
 - Improvement of detection performance is limited

Problem Statement & Background

Exploit coherence between two or more images generated from disparate (location, frequency, resolution, etc.) sonar systems to perform multi-platform underwater target detection

Complications:

- ✓ Variations in operating and environmental conditions with spatially varying clutter
- ✓ Variations in target shapes, compositions, and orientations
- ✓ Lack of a priori knowledge about the shape and geometry of new non-mine-like objects that may be encountered

Problems / Approaches:

- ✓ Single Sensor
 - Limited field of view and targets vary as a function of aspect, grazing angle, and range
 - Improvement of detection performance is limited
- ✓ Disparate Sensors
 - Allow for better capture of target characteristics due to multiple views of the environment
 - Final decision done by post mission analysis (PMA) or network centric analysis (NSA)
 - Collaborative decision making by detecting and isolating the *coherent* information
 - Communication bandwidth is increased, therefore careful design is required

Research Goals & Motivations

Research Goals:

- ✓ Develop a coherence-based detector where the coherent information is found between multiple channels and used to detect objects from sonar imagery with high degree of confidence from one or multiple sonar platforms

Motivations:

- ✓ Coherence analysis between two data channels can be performed by mapping the data to their canonical coordinates and using the canonical correlations. Canonical correlation analysis (CCA) can be used to
 - ✓ Implement the optimum Gauss-Gauss detector
 - ✓ Provide an elegant framework for feature extraction and subsequent classification
 - ✓ Provide the right coordinate system for analysis of coherence between two data channels
 - ✓ Coherence between corresponding region of interest (ROI's) is higher over a target then over background
- ✓ Canonical correlations and coordinates extracted from ROI's are used for *detection*

Sonar Data Sets

Sonar Data Sets

Sonar8:

- ✓ Database contains high frequency side-scan images, consists of envelope data (magnitude of the output of the (k-space / wave-number) beamformer)
- ✓ Contains 512 Images with 293 images containing 310 targets.
- ✓ Set was separated into 3 cases; Easy, Medium, and Hard
 - ✓ **Easy** - low background variation and an overall smooth bottom with targets
 - ✓ **Medium** - contain background clutter and more difficult bottom condition
 - ✓ **Hard** - difficult to detect and classify the targets due to a high variability of background clutter and very difficult bottom conditions

Sonar Data Sets

Sonar8:

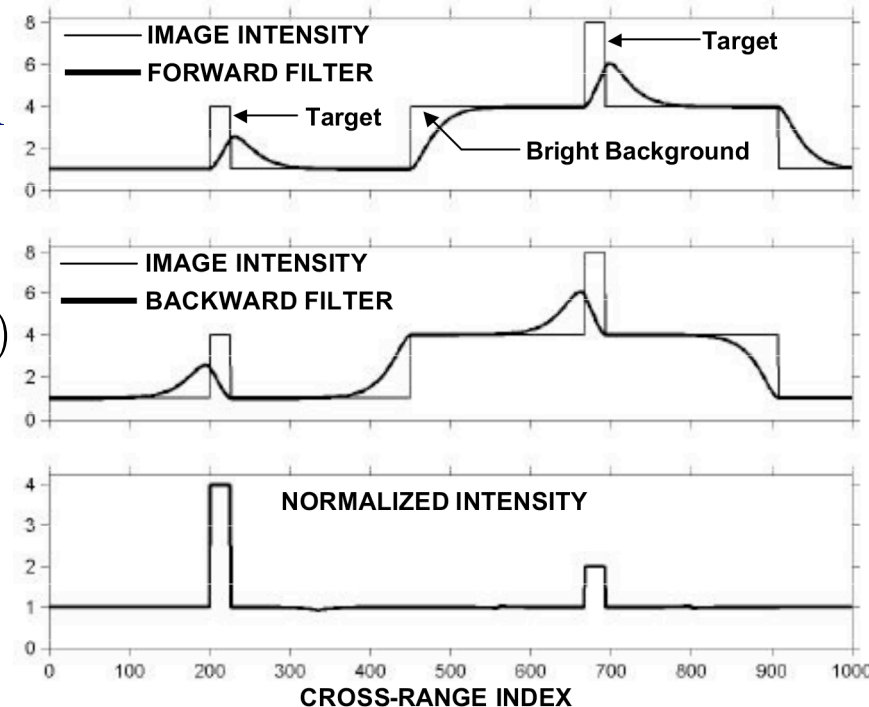
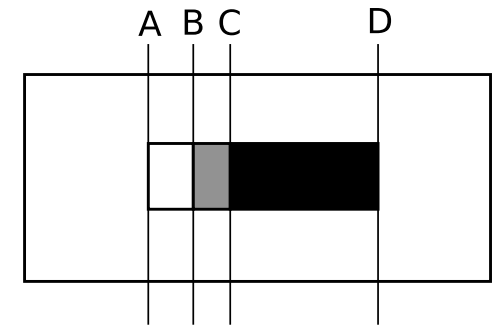
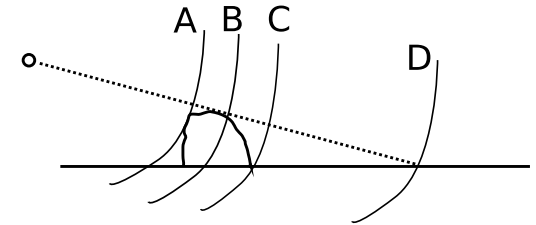
- ✓ Database contains high frequency side-scan images, consists of envelope data (magnitude of the output of the (k-space / wave-number) beamformer)
- ✓ Contains 512 Images with 293 images containing 310 targets.
- ✓ Set was separated into 3 cases; Easy, Medium, and Hard
 - ✓ **Easy** - low background variation and an overall smooth bottom with targets
 - ✓ **Medium** - contain background clutter and more difficult bottom condition
 - ✓ **Hard** - difficult to detect and classify the targets due to a high variability of background clutter and very difficult bottom conditions

Multi-platform:

- ✓ Database contains one high frequency sonar image (HF) and 3 broadband sonar images (BB)
- ✓ Images are complex, direct output of the (k-space / wave-number) beamformer
- ✓ HF offers good target definition, while BB offers reasonable clutter suppression
- ✓ The two sonar systems have different frequency characteristics and yield sonar images with different spatial resolution
- ✓ Database contains 59 Images containing 53 targets

Image Normalization

- ✓ In sonar imagery the target signature consists of bright and dark pixels that make up highlight, dead zone, and shadow
- ✓ Image normalization is used to reduce the variability of the background and to enhance target signature
- ✓ The serpentine forward-backward filter (SFBF) is used (see Dobeck SPIE 2005)
- ✓ The SFBF uses a second-order, low-pass digital filter to generate two estimates of the local background at each processed pixel



$$y(i, j) = c_1 y(i - 1, j - 1) + c_2 y(i - 2, j - 2) + d_0 x(i, j)$$

- ✓ where c_1 , c_2 , and d_0 are the parameters of the filter and depend on the image cross-range resolution and the filter correlation distance

Canonical Coordinate Analysis - An Overview

Two-channel data: $\mathbf{x} \in \mathbb{R}^{m \times 1}$ and $\mathbf{y} \in \mathbb{R}^{n \times 1}$ assume $m \geq n$

Composite covariance matrix: $E \left[\begin{pmatrix} \mathbf{x} \\ \mathbf{y} \end{pmatrix} \begin{pmatrix} \mathbf{x}^H & \mathbf{y}^H \end{pmatrix} \right] = \begin{bmatrix} R_{xx} & R_{xy} \\ R_{yx} & R_{yy} \end{bmatrix}$

SVD of the Coherence Matrix $C = R_{xx}^{-1/2} R_{xy} R_{yy}^{-H/2} = F K G^H$ and $F^H C G = K$,
 $F^H F = I$, $G^H G = I$ where $K = \begin{bmatrix} K(n) \\ 0 \end{bmatrix}$
 $K(n) = \text{diag}[k_1, k_2, \dots, k_n]$

u: Canonical coordinates of \mathbf{x} $\begin{bmatrix} \mathbf{u} \\ \mathbf{v} \end{bmatrix} = \begin{bmatrix} F^H & 0 \\ 0 & G^H \end{bmatrix} \begin{bmatrix} R_{xx}^{-1/2} & 0 \\ 0 & R_{yy}^{-1/2} \end{bmatrix} \begin{bmatrix} \mathbf{x} \\ \mathbf{y} \end{bmatrix}$
v: Canonical coordinates of \mathbf{y}

Composite covariance matrix of **u** and **v**:

$$E \left[\begin{pmatrix} \mathbf{u} \\ \mathbf{v} \end{pmatrix} \begin{pmatrix} \mathbf{u}^H & \mathbf{v}^H \end{pmatrix} \right] = \begin{bmatrix} R_{uu} & R_{uv} \\ R_{vu} & R_{vv} \end{bmatrix} = \begin{bmatrix} I & K \\ K & I \end{bmatrix},$$

The diagonal matrix K is the **canonical correlation matrix** of canonical correlations $k_i, i = 1 : n$

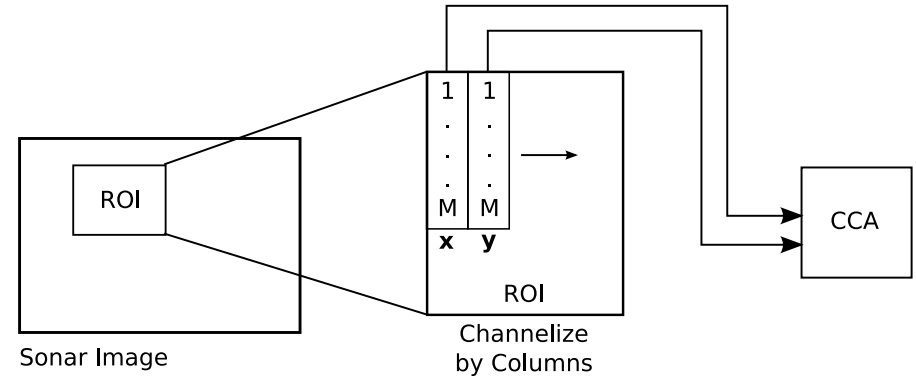
The top N diagonal elements of K (arranged in descending order) are used for **detection**.

Data Extraction for CCA

Data Extraction for CCA

Single Sensor

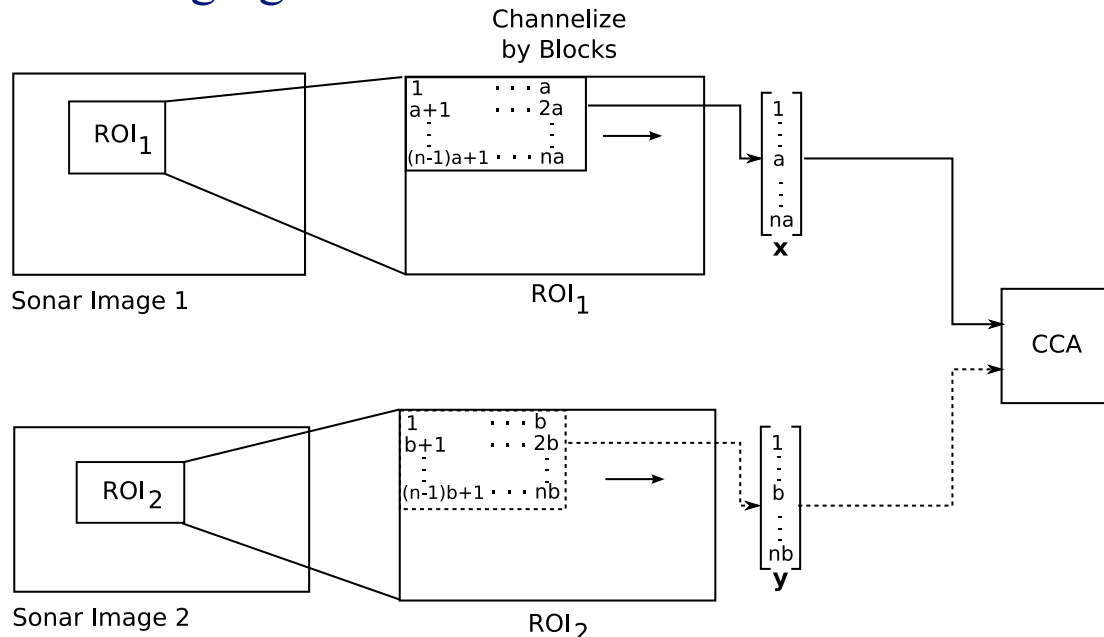
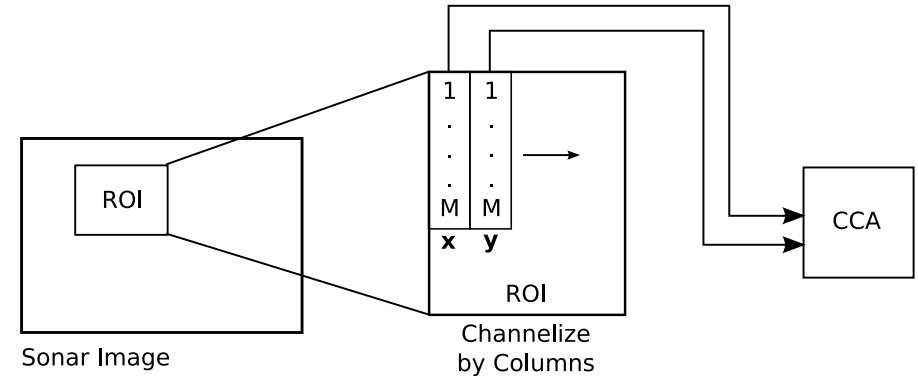
- ✓ Each image was then partitioned into $M \times N$ Region of Interests (ROI's) of size 46×180 experimentally determined based on average target size
- ✓ 50% overlapping to avoid splitting of target amongst ROI's
- ✓ Each ROI is then channelized column-wise (30-dimensional) with 50% channel overlap
- ✓ Averaging done overall all columns



Data Extraction for CCA

Single Sensor

- ✓ Each image was then partitioned into $M \times N$ Region of Interests (ROI's) of size 46×180 experimentally determined based on average target size
- ✓ 50% overlapping to avoid splitting of target amongst ROI's
- ✓ Each ROI is then channelized column-wise (30-dimensional) with 50% channel overlap
- ✓ Averaging done overall all columns



Dual Disparate Sensor

- ✓ Each image was then partitioned, with 50% overlap, into $M \times N$ ROI's of size 72×112 for HF and 24×224 for BB, which were experimentally determined based on average target size.
- ✓ Each ROI is then channelized block-wise (6×4 for HF) and (2×8 for BB)
- ✓ Averaging done over all blocks

Gauss - Gauss Detection

- ✓ The log-likelihood ratio that minimizes the risk involved in deciding between $H_0 : R = R_0$ i.e. noise alone, vs $H_1 : R = R_1 = R_s + R_0$, i.e. signal plus noise

$$\gamma(\mathbf{x}) = \begin{cases} 1 \sim H_1, & l(\mathbf{x}) > \eta \\ 0 \sim H_0, & l(\mathbf{x}) \leq \eta \end{cases}$$

$$l(\mathbf{x}) = \mathbf{x}^H \mathbf{Q} \mathbf{x} \text{ with } \mathbf{Q} = R_0^{-1} - R_1^{-1}$$

\mathbf{Q} can be decomposed into, $\mathbf{Q} = R_0^{-H/2} (\mathbf{I} - \mathbf{S}^{-1}) R_0^{-1/2}$, $\mathbf{S} = R_0^{-1/2} R_1 R_0^{-H/2}$ where \mathbf{S} is the “signal-to-noise ratio” matrix

The J-divergence which is a measure of separability, $J = E_{H_1} [l(\mathbf{x})] - E_{H_0} [l(\mathbf{x})]$

$$J = \text{tr}(\mathbf{S} + \mathbf{S}^{-1} - 2\mathbf{I})$$

Decompose $\mathbf{S} = \mathbf{U} \mathbf{\Lambda} \mathbf{U}^H$

$$J = \sum_{i=1}^m (\lambda_i + \lambda_i^{-1} - 2) \quad \text{and} \quad l(\boldsymbol{\xi}) = \boldsymbol{\xi}^H \mathbf{U} (\mathbf{I} - \mathbf{\Lambda}^{-1}) \mathbf{U}^H \boldsymbol{\xi} \quad , \text{ where } \boldsymbol{\xi} = R_0^{-1/2} \mathbf{x}$$

CCA-Based Detection

Implements the Gauss-Gauss detector for testing between $H_0 : \mathbf{y} = \mathbf{n} : CN_n[0, R_0]$ i.e. noise alone versus $H_1 : \mathbf{y} = \mathbf{s} + \mathbf{n} : CN_n[0, R_1 = R_s + R_0]$ i.e. signal plus noise

The log-likelihood in CCA

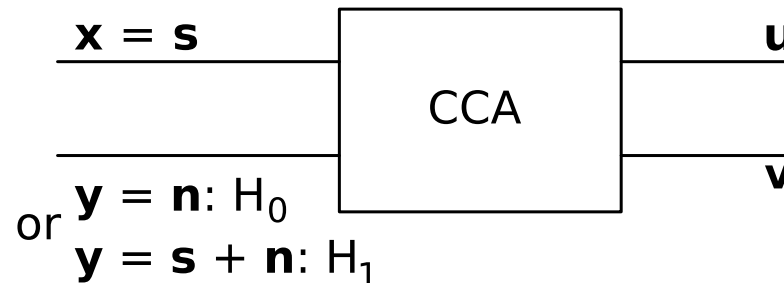
$$l(\mathbf{v}) = \mathbf{v}^H ([I - K^2]^{-1} - I) \mathbf{v}$$

leads to J-divergence test which is a measure of separability

$$J = E_{H_1}[l(\mathbf{v})] - E_{H_0}[l(\mathbf{v})] = tr([I - K^2]^{-1} - I - K^2)$$

$$J_r = \sum_{i=1}^r \frac{k_i^4}{1 - k_i^2}$$

i.e. the rank- r detector that maximizes J-divergence uses the *dominant* canonical correlations



Dual Disparate Sonar Target Detection

To perform target detection in dual sonar imagery with possibly different properties the hypothesis testing involves

$$H_0 : \begin{bmatrix} \mathbf{x} \\ \mathbf{y} \end{bmatrix} = \begin{bmatrix} \mathbf{n}_1 \\ \mathbf{n}_2 \end{bmatrix} \text{ and } H_1 : \begin{bmatrix} \mathbf{x} \\ \mathbf{y} \end{bmatrix} = \begin{bmatrix} \mathbf{s} + \mathbf{n}_1 \\ \mathbf{s} + \mathbf{n}_2 \end{bmatrix} \text{ with}$$

$$\bar{R}_0 = \begin{bmatrix} R_0 & 0 \\ 0 & R_0 \end{bmatrix} \text{ and } \bar{R}_1 = \begin{bmatrix} R_s + R_0 & R_s \\ R_s & R_s + R_0 \end{bmatrix}$$

This leads to the following new log-likelihood and J-divergence (detectability measure) as

$$l(\mathbf{w}) = \mathbf{w}^H \begin{bmatrix} 1/2I - 1/4(K^{-2} - 1/2I)^{-1} & 1/2K^{-1} - 1/4(K^{-1} - 1/2K)^{-1} \\ 1/2K^{-1} - 1/4(K^{-1} - 1/2K)^{-1} & 1/2K^{-2} - 1/4(I - 1/2K^2)^{-1} \end{bmatrix} \mathbf{w}$$

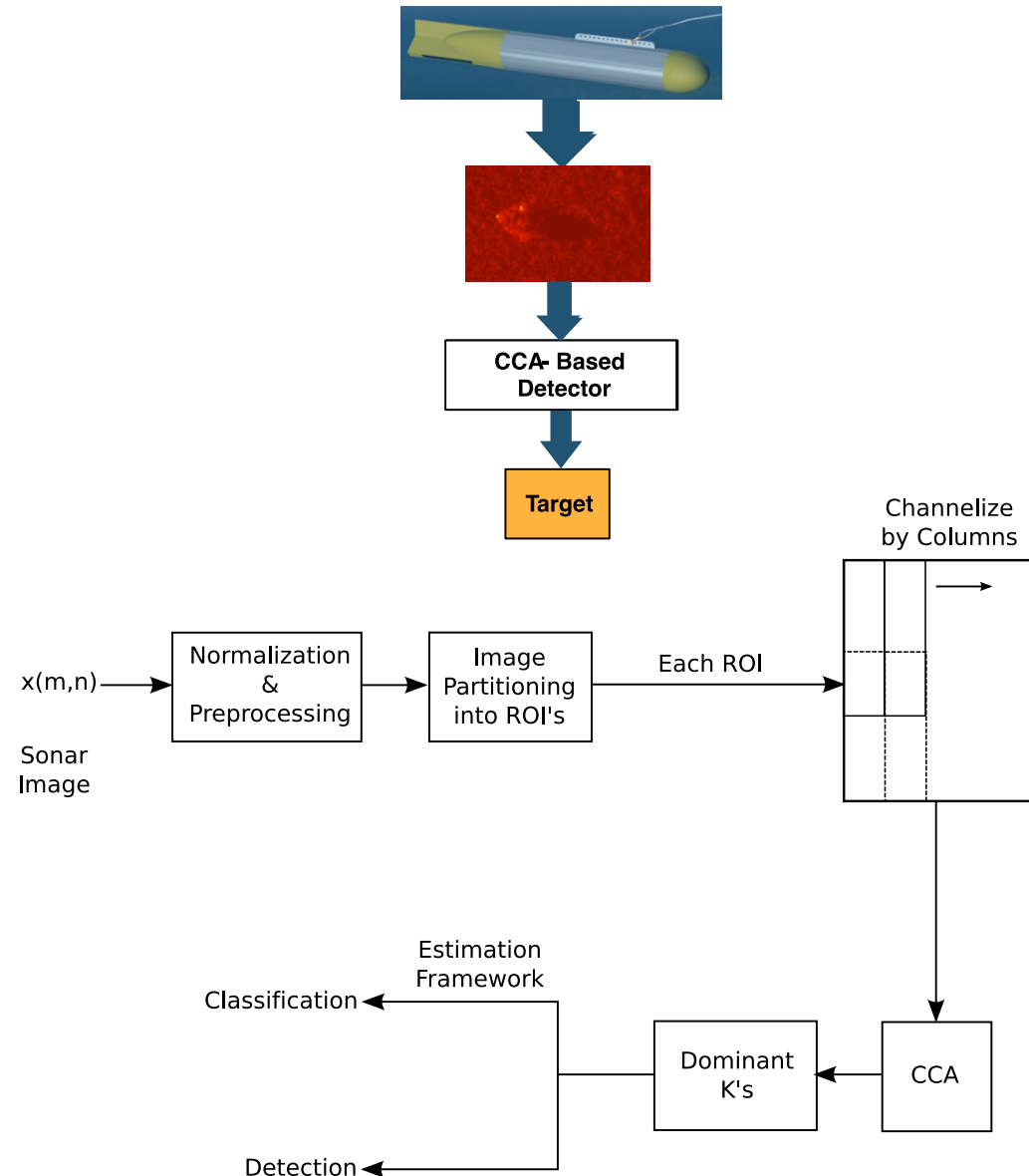
where \mathbf{w} is the composite canonical coordinate vector

$$J_r = \sum_{i=1}^r -2 + \frac{4}{1 - k_i^4}$$

i.e. the rank- r detector that maximizes J-divergence uses the *dominant* canonical correlations

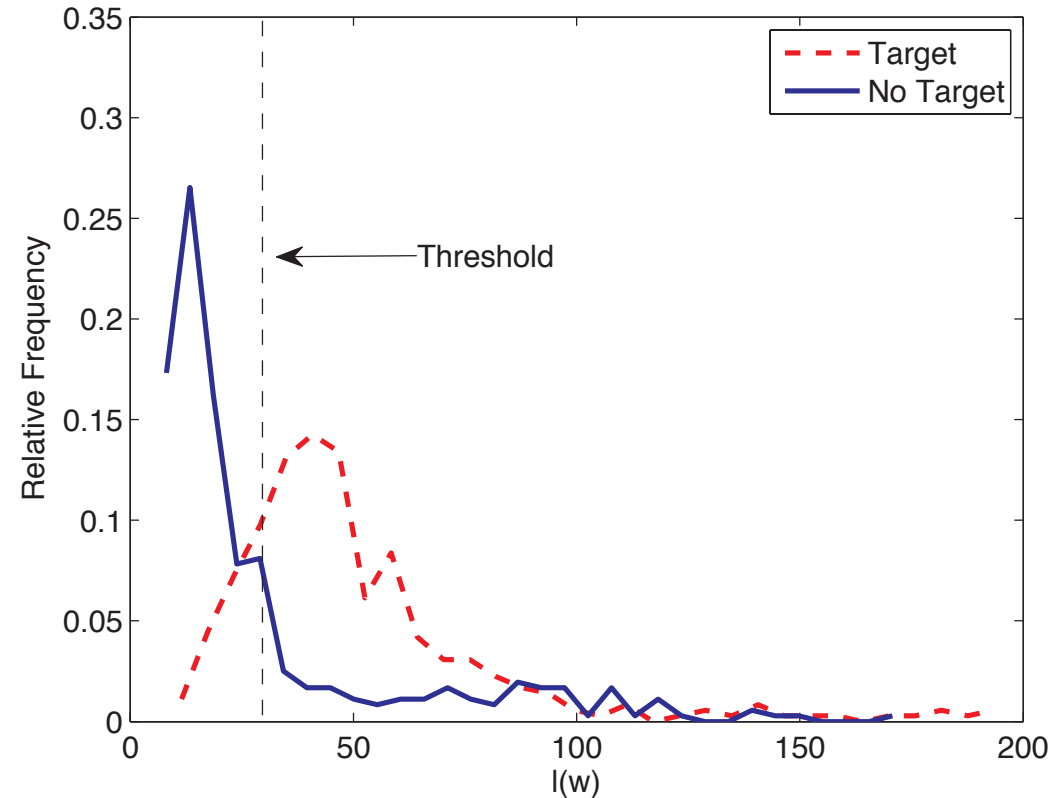
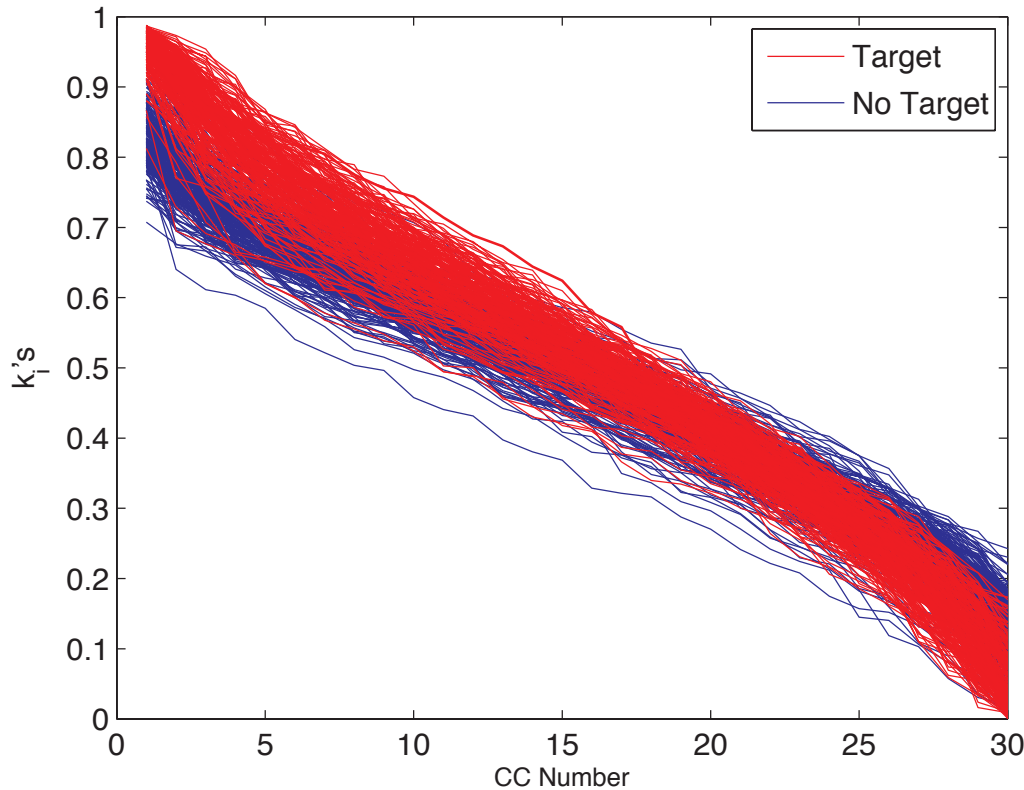
Single Sensor Case

- ✓ Images are normalized using SFBF normalizer
- ✓ Each image was then partitioned into ROI's of size 46 x 180, with 50% overlap
- ✓ Channelized in a column-wise with dimension 30 pixels
- ✓ Consecutive columns in a ROI are more coherent when a target is present compared to when there is background only
- ✓ After the channels are formed, the J-divergence is computed, and the log-likelihood is computed for each pair of columns
- ✓ If 50% of the column pairs are greater than the detection threshold, the ROI is flagged as a target
- ✓ Evaluated on Sonar8 data set



Results on Sonar8

Canonical Correlation for Sample Target/Non Target Set



- ✓ To show the separability of the dominant canonical correlations a test was conducted on the entire target set and a same size random set of backgrounds
- ✓ Dominant (top 10) canonical correlations exhibit good separability, i.e. more coherence between x and y over a target versus background, hence providing better detectability
- ✓ Based upon the test set a threshold of 38.2 was experimentally determined

Results on Sonar8

Easy Cases

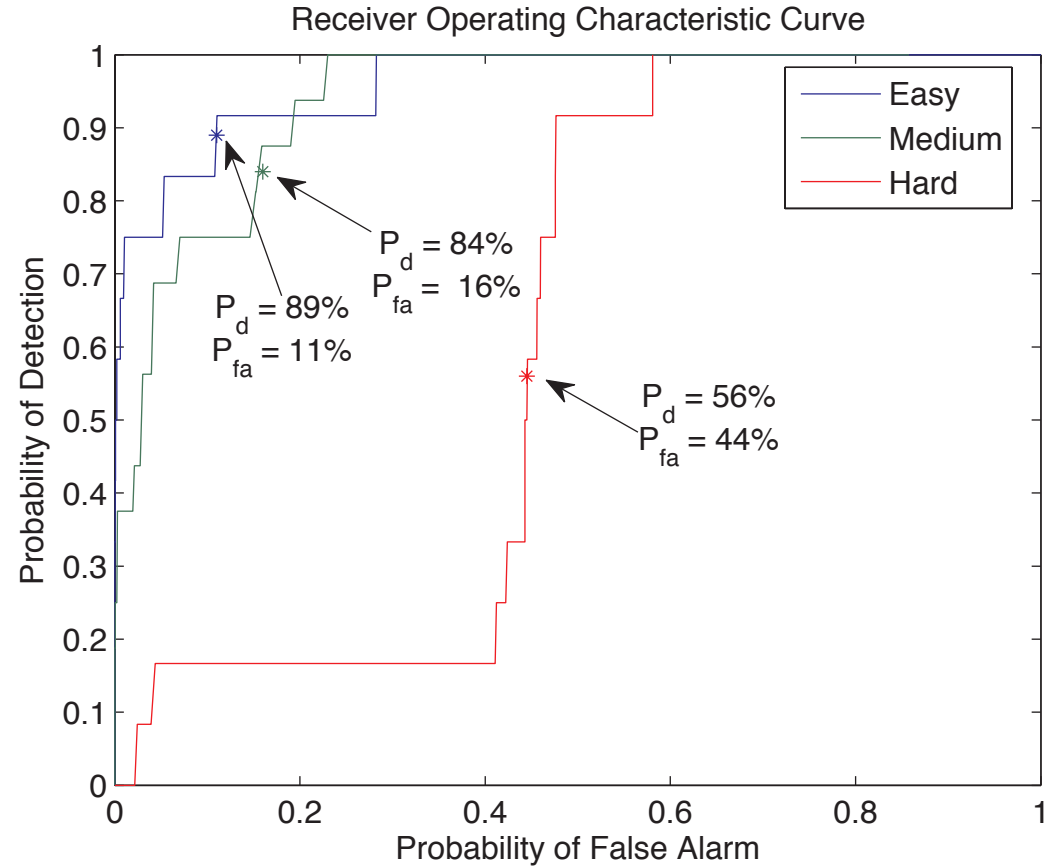
- 106 Images containing 233 Targets
- Detected 229 Targets
- Averaged 19 False Alarms per image
- Knee Point $P_d = 89\%$ / $P_{fa} = 11\%$

Medium Cases

- 29 Images containing 49 Targets
- Detected 43 Targets
- Averaged 22 False Alarms per image
- Knee Point $P_d = 84\%$ / $P_{fa} = 16\%$

Hard Cases

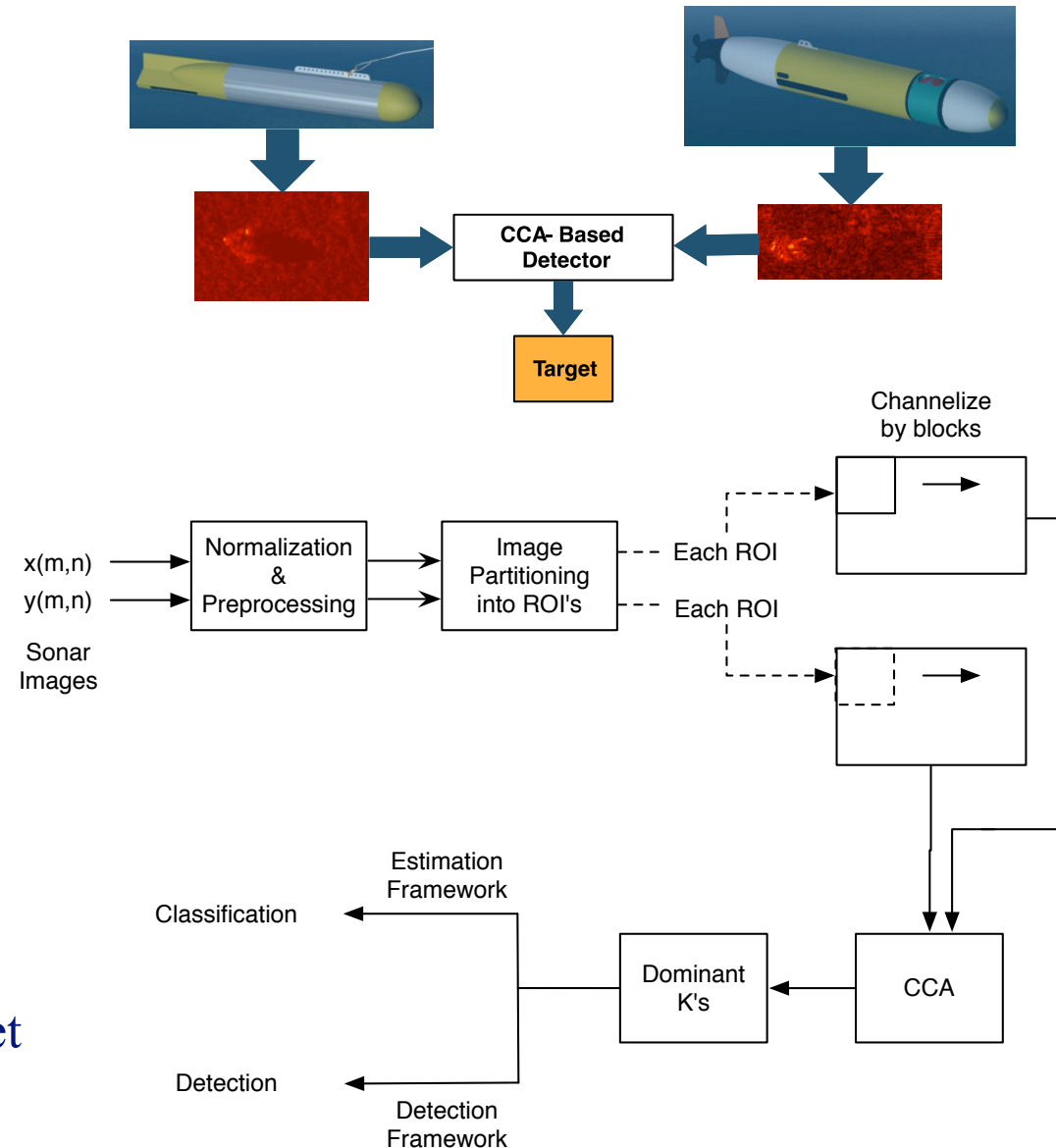
- 2 Images containing 4 Targets
- Detected 3 Targets
- Averaged 30 False Alarms per image
- Knee Point $P_d = 56\%$ / $P_{fa} = 44\%$



- ✓ Difficult to generalize the hard case due to small number of targets
- ✓ Overall good detection results, false alarms per image are rather high

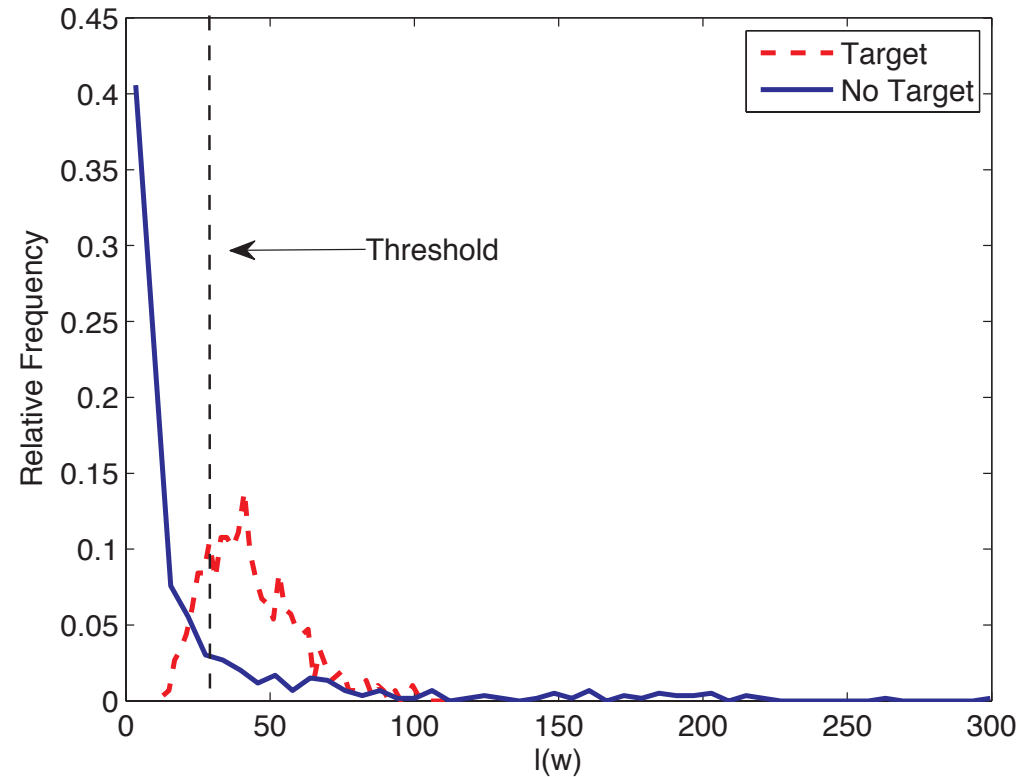
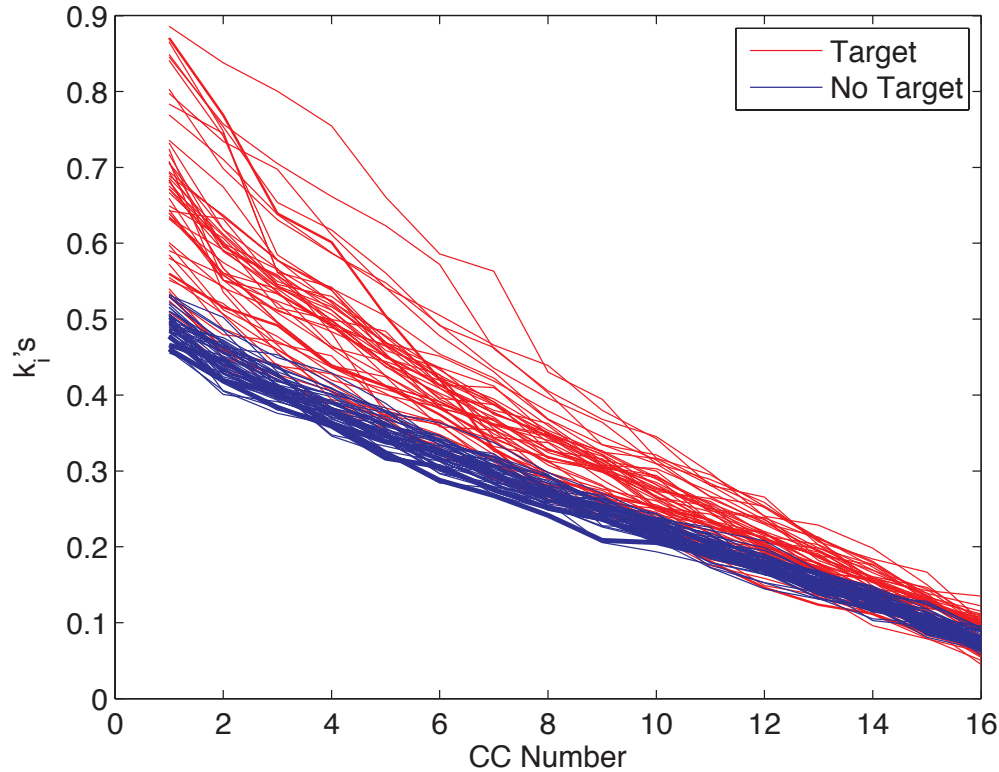
Dual Disparate Case

- ✓ Each image was then partitioned into ROI's of size 72 x 112 for HF and 24 x 224 for BB, with 50% overlap
- ✓ Each ROI is then channelized block-wise (6 x 4 for HF) and (2 x 8 for BB)
- ✓ Pair of blocks from a pair of ROI's are more coherent when a target is present compared to when there is background only
- ✓ After the channels are formed, the J-divergence is computed, and the log-likelihood is computed for each pair of blocks
- ✓ If 50% of the blocks are greater than the detection threshold, the ROI is flagged as a target
- ✓ Evaluated on Multi-platform sonar data set with disparateness in frequency



Results on HF-BB Detection

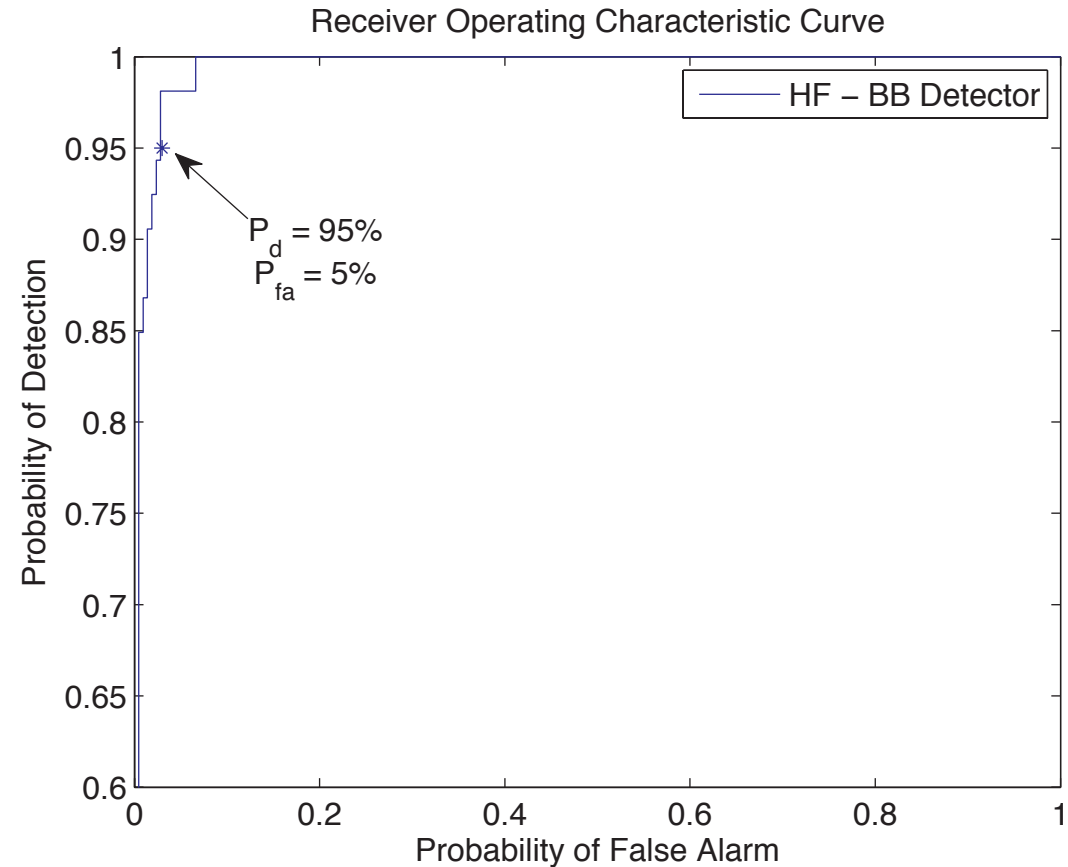
Canonical Correlation for Sample Target/Non Target Set



- ✓ To show the separability of the dominant canonical correlations a test was conducted on the entire target set and a same size random set of backgrounds
- ✓ Dominant (top 8) canonical correlations exhibit good separability, i.e. more coherence between x and y over a target versus background
- ✓ Based upon the test set a detection threshold of 26.4 of the HF - BB detector

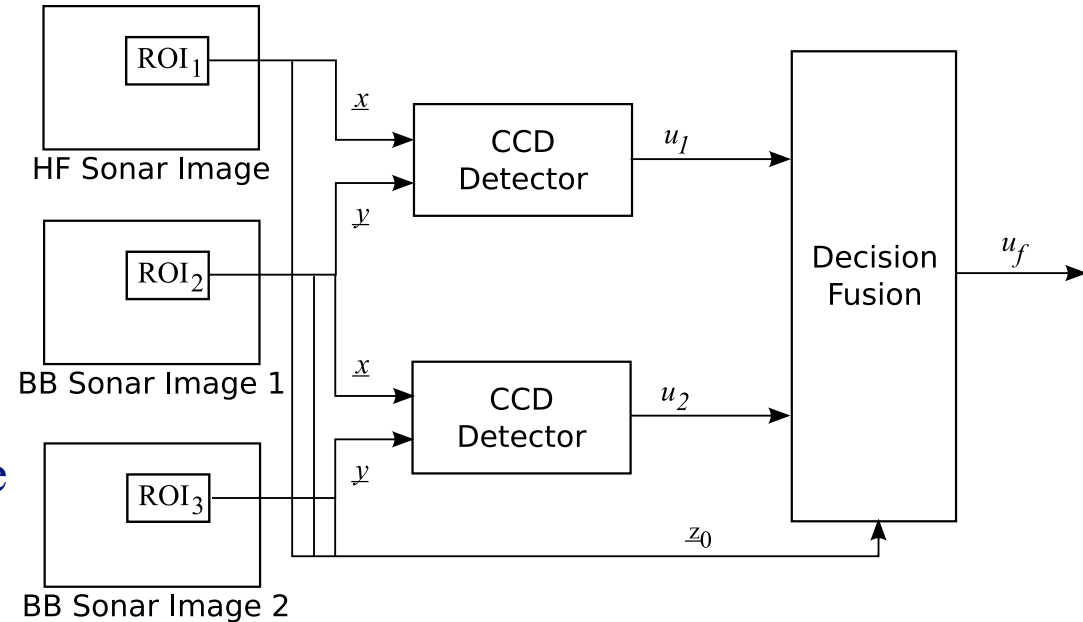
Results on HF-BB Detection

- ✓ 51 of the 53 targets were detected with an average of 10 false alarms per image
- ✓ The knee point on the ROC Curve $P_d = 95\% / P_{fa} = 5\%$
- ✓ Missed targets consisted were at very close range and near the AUV path
- ✓ Moreover the missed targets were barely visible and extremely dark in the HF and barely a bright spot in the BB image
- ✓ Therefore there was a low coherence between the pair of ROI's
- ✓ Overall, the detector performed extremely well given the small number of targets and non-targets used to form the detection threshold.



Distributed Detection

- ✓ The use of more than one decision on the environment can improve results
- ✓ The first detector checks for coherence across two broadbands, while the second one reconfirms presence of an object in both high frequency and broadband images
- ✓ A Fusion is used to improve the confidence of the decisions
- ✓ Fusion Rule



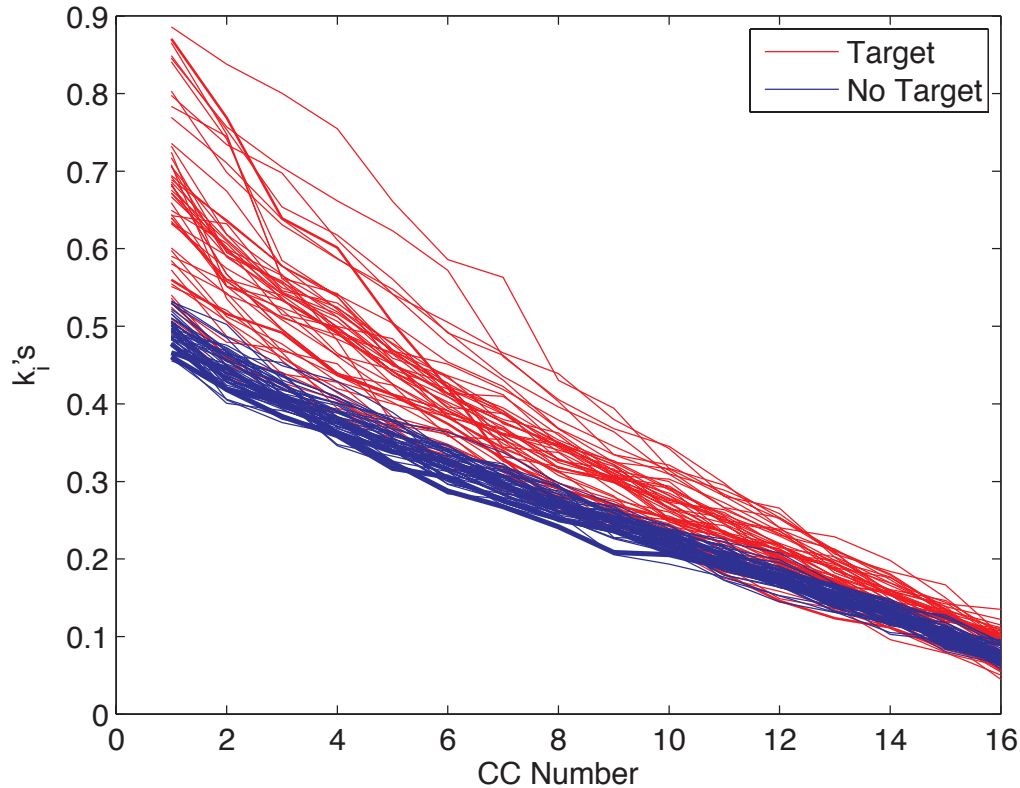
$$\gamma_f(u_1, \dots, u_N, \mathbf{z}_0) = \frac{p(\mathbf{z}_0|H_1) \prod_{i=1}^N p(u_i|H_1)}{p(\mathbf{z}_0|H_0) \prod_{i=1}^N p(u_i|H_0)} \underset{H_0}{\overset{H_1}{\geq}} \lambda \text{ with threshold } \lambda = \frac{P_0 [C_{10} - C_{00}]}{P_1 [C_{01} - C_{11}]}$$

- ✓ \mathbf{z}_0 : independent observation of fusion center, for our implementation these are statistical descriptors of the 3 ROI's (mean, skew, and variance)

$\frac{p(\mathbf{z}_0 H_1)}{p(\mathbf{z}_0 H_0)}$	found using a probabilistic neural network	$\frac{\prod_{i=1}^N p(u_i H_1)}{\prod_{i=1}^N p(u_i H_0)}$	found using a back-propagation neural network
---------------------------------------------------	--------------------------------------------	-------------------------------------------------------------	-----------------------------------------------

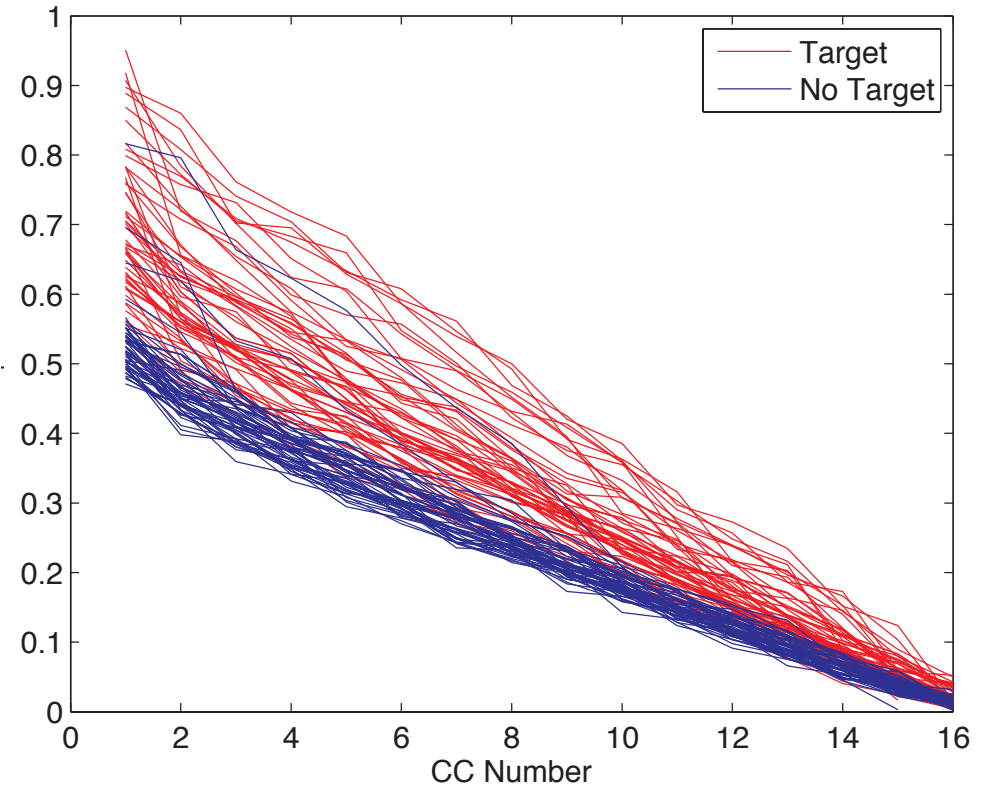
Distributed Detection Results

Canonical Correlation for Sample Target/Non Target Set



HF - BB₁

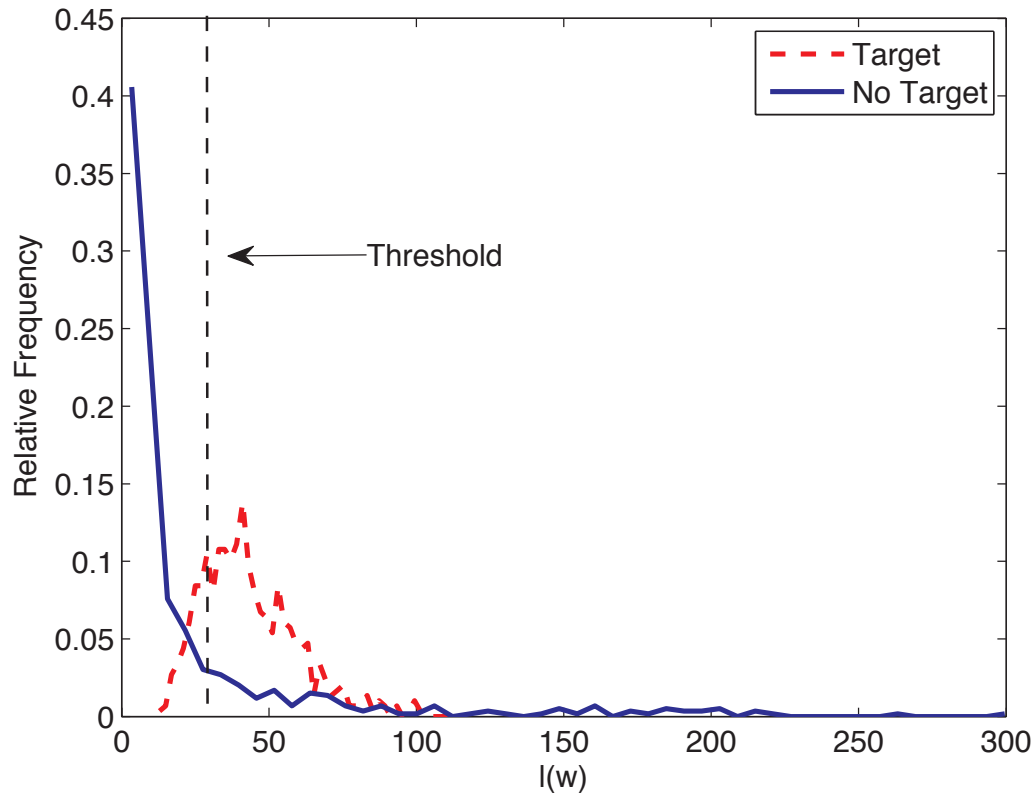
Canonical Correlation for Sample Target/Non Target Set



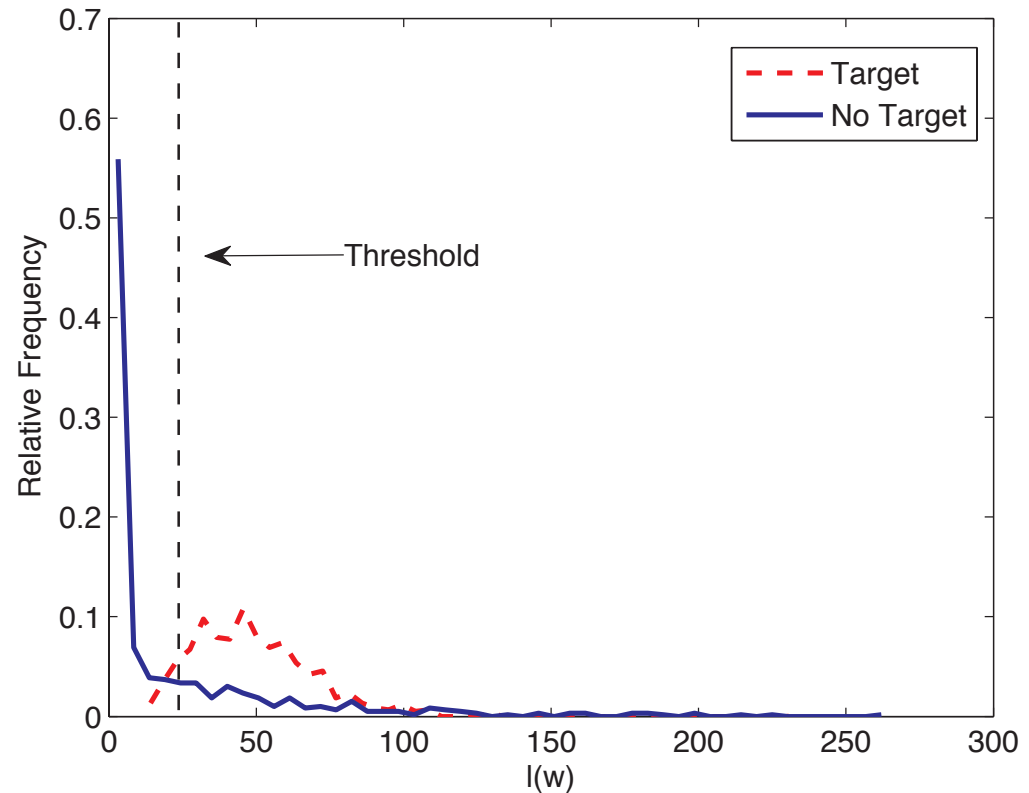
BB₁ - BB₂

- ✓ To show the separability of the dominant canonical correlations a test was conducted on the entire target set and a same size random set of backgrounds for both detectors
- ✓ Better separation between target and non-target for HF-BB₁, but overall good separation between two hypotheses

Distributed Detection Results



HF - BB₁

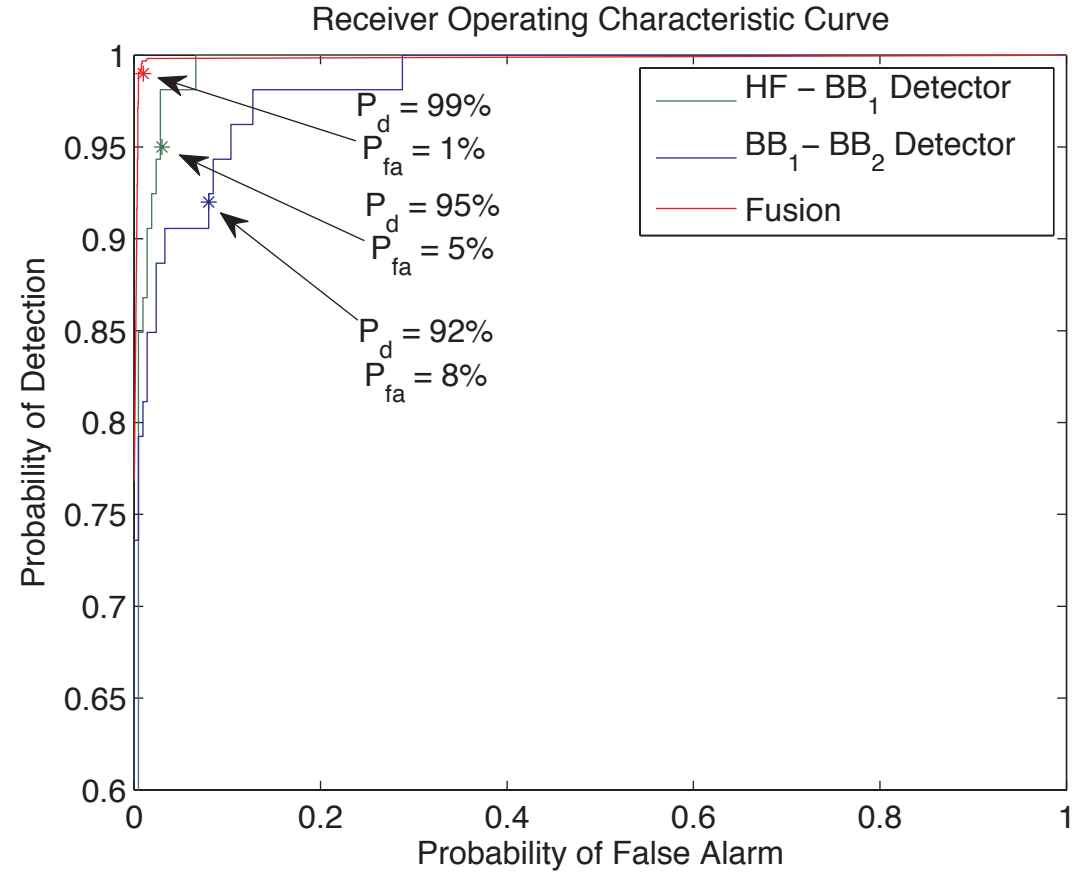


BB₁ - BB₂

- ✓ Based upon the test set a threshold of 26.4 for the HF-BB₁ and 23.9 for the BB₁-BB₂, was experimentally determined

Detection Results

- ✓ Targets are detected with high probability and low false alarm rates.
- ✓ **HF - BB₁**
- ✓ 51 of the 53 targets were detected with an average of 10 false detections per image.
- ✓ Knee Point $P_d = 95\% / P_{fa} = 5\%$
- ✓ **BB₁ - BB₂**
- ✓ 49 of the 53 targets were detected with an average of 9 false detections per image.
- ✓ Knee Point $P_d = 92\% / P_{fa} = 8\%$
- ✓ **Fusion**
- ✓ 53 of the 53 targets were detected with an average of 7 false detections per image.
- ✓ Fusion Knee Point $P_d = 99\% / P_{fa} = 1\%$



- ✓ Considering the threshold was determined on such a small set of backgrounds the detector performs extremely well.

Sample Support of Gauss-Gauss Detection

The covariance matrices are estimated from a limited number of data samples

Consider the sample data matrices $X = [\mathbf{x}_1, \mathbf{x}_2, \dots, \mathbf{x}_M] \in \mathbb{R}^{m \times M}$

$Y = [\mathbf{y}_1, \mathbf{y}_2, \dots, \mathbf{y}_M] \in \mathbb{R}^{m \times M}$

Sample Support of Gauss-Gauss Detection

The covariance matrices are estimated from a limited number of data samples

Consider the sample data matrices $X = [\mathbf{x}_1, \mathbf{x}_2, \dots, \mathbf{x}_M] \in \mathbb{R}^{m \times M}$

$Y = [\mathbf{y}_1, \mathbf{y}_2, \dots, \mathbf{y}_M] \in \mathbb{R}^{m \times M}$

Sample Rich Case $m \leq M$

Sampled signal-to-noise ratio matrix $\hat{S} = (X X^H)^{-1/2} (Y Y^H) (X X^H)^{-H/2} = U \Lambda U^H$

Decompose eigenvalue problem $(Y Y^H) D = (X X^H) D \Lambda$ where $D \triangleq (X X^H)^{-H/2} U$

Log-Likelihood $l(\mathbf{x}) = \mathbf{x}^H D (I - \Lambda^{-1}) D^H \mathbf{x}$ $J = \sum_{i=1}^m (\lambda_i + \lambda_i^{-1} - 2)$

Sample Support of Gauss-Gauss Detection

The covariance matrices are estimated from a limited number of data samples

Consider the sample data matrices $X = [\mathbf{x}_1, \mathbf{x}_2, \dots, \mathbf{x}_M] \in \mathbb{R}^{m \times M}$

$Y = [\mathbf{y}_1, \mathbf{y}_2, \dots, \mathbf{y}_M] \in \mathbb{R}^{m \times M}$

Sample Rich Case $m \leq M$

Sampled signal-to-noise ratio matrix $\hat{S} = (X X^H)^{-1/2} (Y Y^H) (X X^H)^{-H/2} = U \Lambda U^H$

Decompose eigenvalue problem $(Y Y^H) D = (X X^H) D \Lambda$ where $D \triangleq (X X^H)^{-H/2} U$

Log-Likelihood $l(\mathbf{x}) = \mathbf{x}^H D (I - \Lambda^{-1}) D^H \mathbf{x}$ $J = \sum_{i=1}^m (\lambda_i + \lambda_i^{-1} - 2)$

Sample Poor Case $m > M$

Sampled signal-to-noise ratio matrix will be of p , due to $rank(X X^H) = p \leq M$

$\hat{S}_p = (V_{1,p} \Lambda_X^2(p) V_{1,p}^H)^{-1/2} (W_{1,p} \Lambda_Y^2(p) W_{2,p}^H) (V_{1,p} \Lambda_X^2(p) V_{1,p}^H)^{-H/2} = U_p \Lambda(p) U_p^H$

Decompose eigenvalue problem $(X^H Y)(Y^H X) A_p = (X^H X)(X^H X) A_p \Lambda(p)$

Log-Likelihood $l(\mathbf{x}) = \mathbf{x}^H X (I - A_p \Lambda^{-1}(p) A_p^H) X^H \mathbf{x}$

Kernel Gauss - Gauss Detection

Define the mapped data matrices $\Phi = [\phi(\mathbf{x}_1), \phi(\mathbf{x}_2), \dots, \phi(\mathbf{x}_M)] \in \mathbb{R}^{m' \times M}$

$\Psi = [\phi(\mathbf{y}_1), \phi(\mathbf{y}_2), \dots, \phi(\mathbf{y}_M)] \in \mathbb{R}^{m' \times M}$ where $m' \geq m$

mapped using high-dimensional kernel producing mapping function of $\phi(\cdot)$

Using sample poor derivations, which is already dot product form we can write the log-likelihood as

$$l(\phi(\mathbf{x})) = \mathbf{k}_{\phi\Phi}^H (I - A_\phi \Lambda_\phi^{-1} A_\phi^H) \mathbf{k}_{\phi\Phi} \quad J = \sum_{i=1}^m (\lambda_i + \lambda_i^{-1} - 2)$$

where $\mathbf{k}_{\phi\Phi} = \phi^H(\mathbf{x})\Phi = [k(\mathbf{x}, \mathbf{x}_1), \dots, k(\mathbf{x}, \mathbf{x}_M)]^H$ and $k(\mathbf{x}, \mathbf{x}_i) = \phi^H(\mathbf{x})\phi(\mathbf{x}_i)$ is a kernel function that satisfies Mercer's conditions

Matrices can be found by solving the generalized eigenvalue problem

$$K_{\Phi\Psi} K_{\Phi\Psi}^H A_\phi = K_{\Phi\Phi} K_{\Phi\Phi} A_\phi \Lambda_\phi$$

where $K_{\Phi\Psi} = \Phi^H \Psi = [k(\mathbf{x}_i, \mathbf{y}_j)]_{ij}$ and $K_{\Phi\Phi} = \Phi^H \Phi = [k(\mathbf{x}_i, \mathbf{x}_j)]_{ij}$ are the Gram kernel matrices

Linear Simulation

✓ Shows the effectiveness of the detector for the sample rich and the sample poor cases

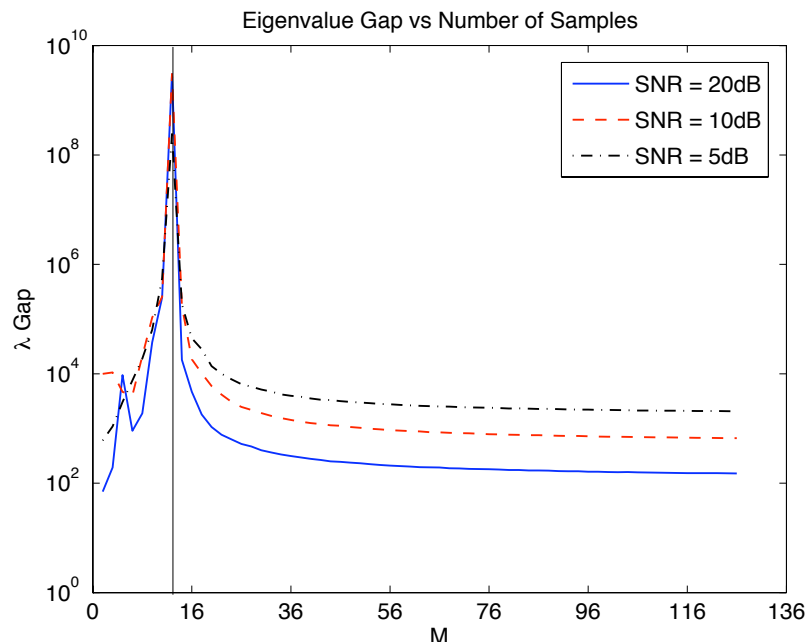
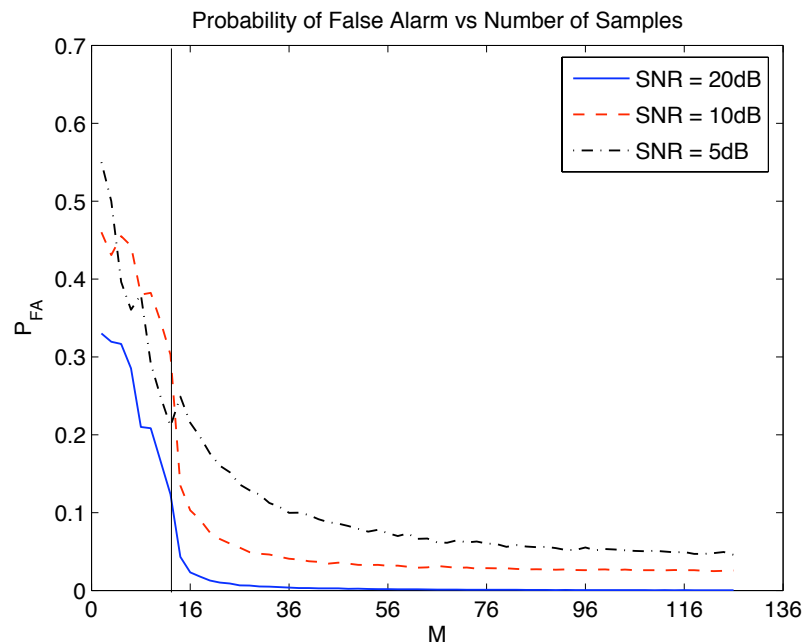
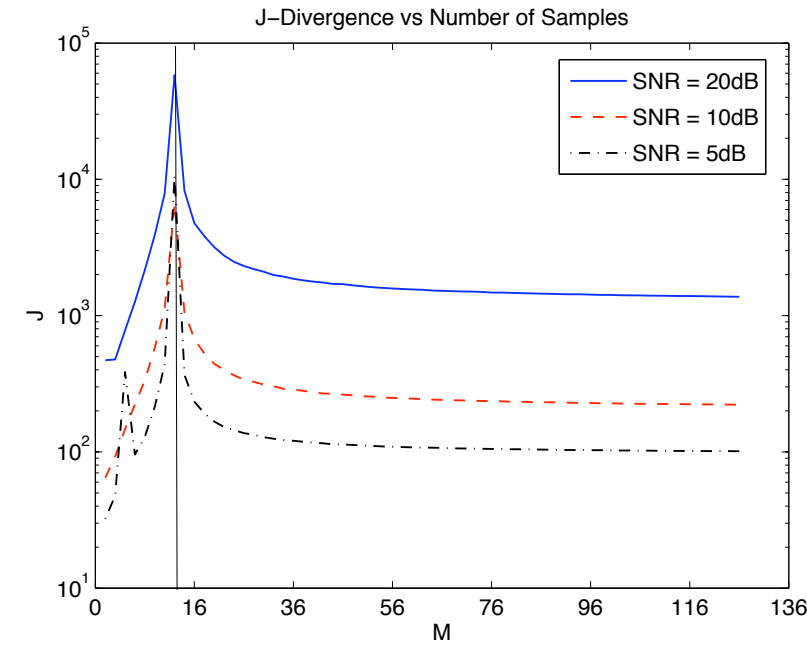
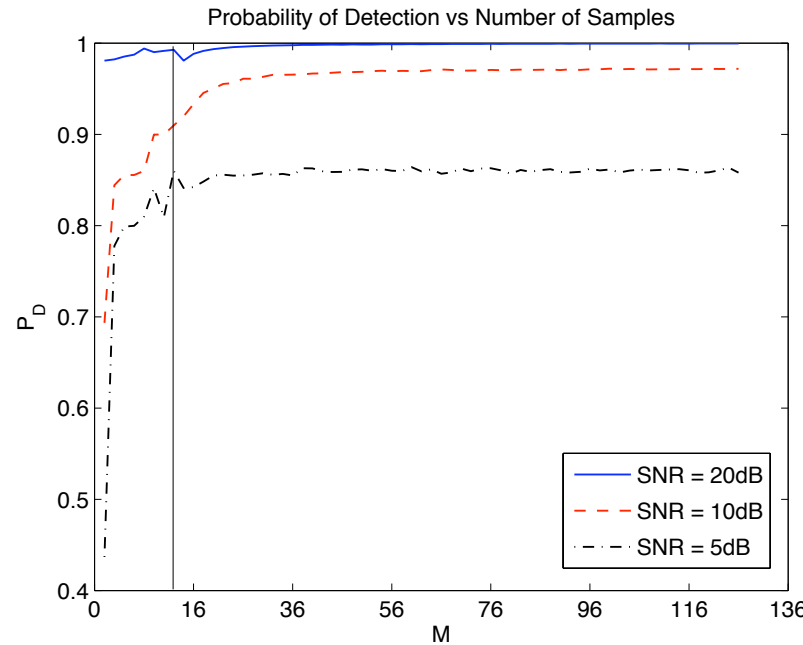
✓ Signal Model

$$y = B\eta + n$$

$$R_\eta = 1.25I$$

$$m = 12$$

✓ The eigenvalues of the signal-to-noise ratio matrix become defective and the empirical J-divergence is defective



Conclusions

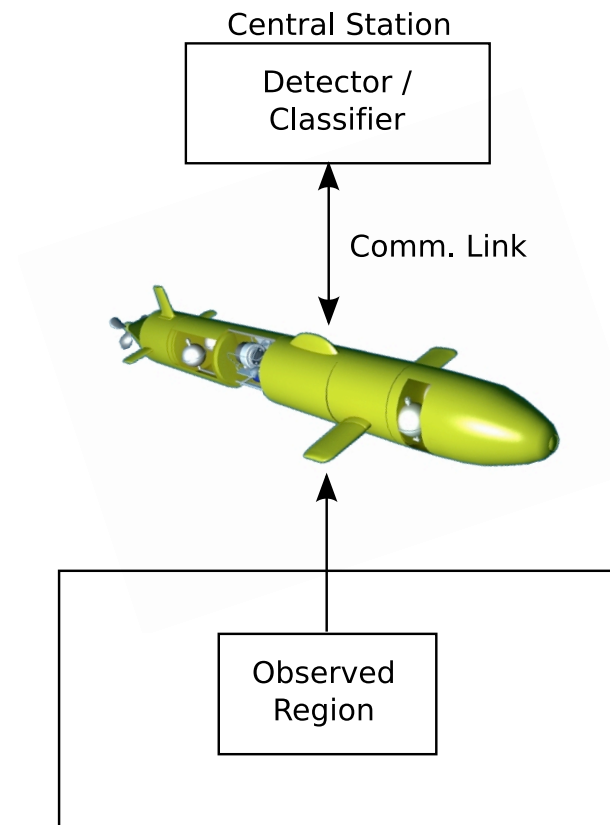
- ✓ An optimum Gauss-Gauss-based detector for detection of targets in multiple disparate sonar imagery is developed. The basic idea is to exploit coherence-based properties in the ROIs of the sonar images
- ✓ Experimental results on NSWC database demonstrated that dominant canonical correlations extracted over one ROI or pairs of ROI's of sonar images lead to good separability between targets and non-targets
- ✓ Dual disparate platform detection performed the best with 10 false alarms per image and two missed detections
- ✓ Distributed detection can be used to further improve the detection performance to 7 false alarms per image and no missed detections
- ✓ Studied the sample support of Gauss-Gauss detection, as sample support becomes poor the J-divergence measure becomes defective
- ✓ Any kernel implementation needs to have a large sample support

Future Work

- ✓ Extend the 2-channel Gauss-Gauss detector to M -channels to allow for more platforms to be used simultaneously
 - Multi-channel coherence analysis (MCA) offers a beautiful framework for finding coherence between 2 or more channels
- ✓ Extension from two hypothesis to M -hypothesis to handle the cases where only one sensor contains the target
- ✓ Extend the distributed detection system to include collaboration between the local decision makers, similar to the developed CMAC
- ✓ Applications to other sensory modalities, e.g. magnetic, electro-optical, etc
- ✓ The main development in this work concentrated on the detection aspect of the problem. The next natural step would be the development and study of a classification system
 - canonical correlations that are used for detection can also be used as feature vectors for input to a classifier

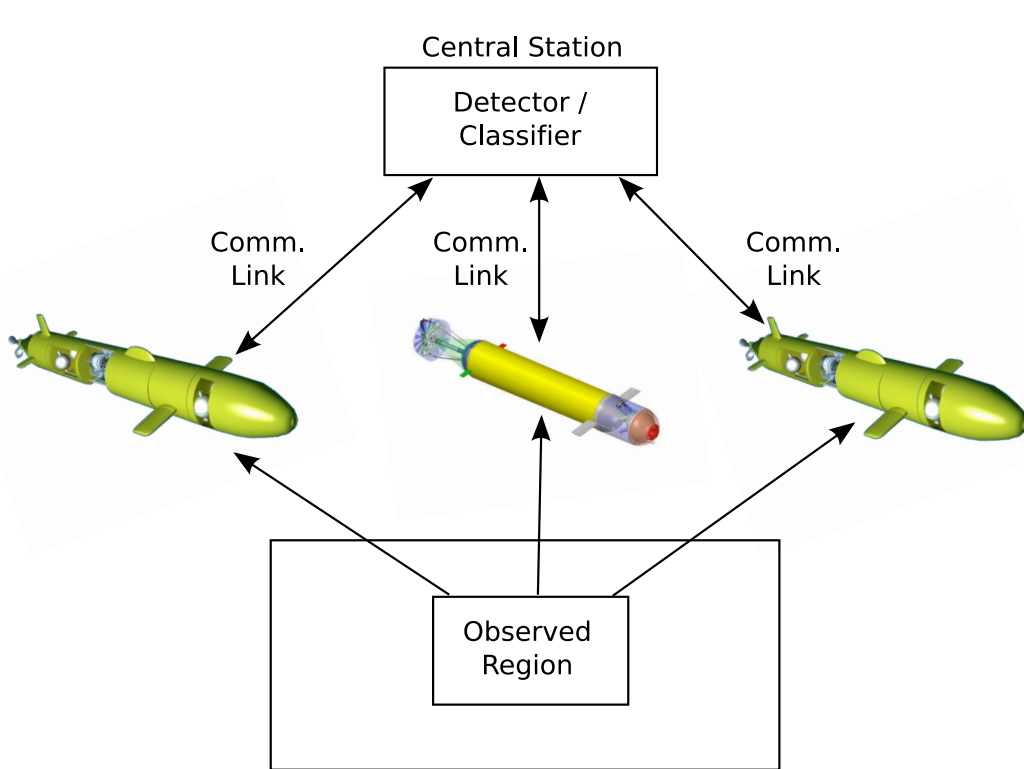
Questions ?

Single Sensor Case

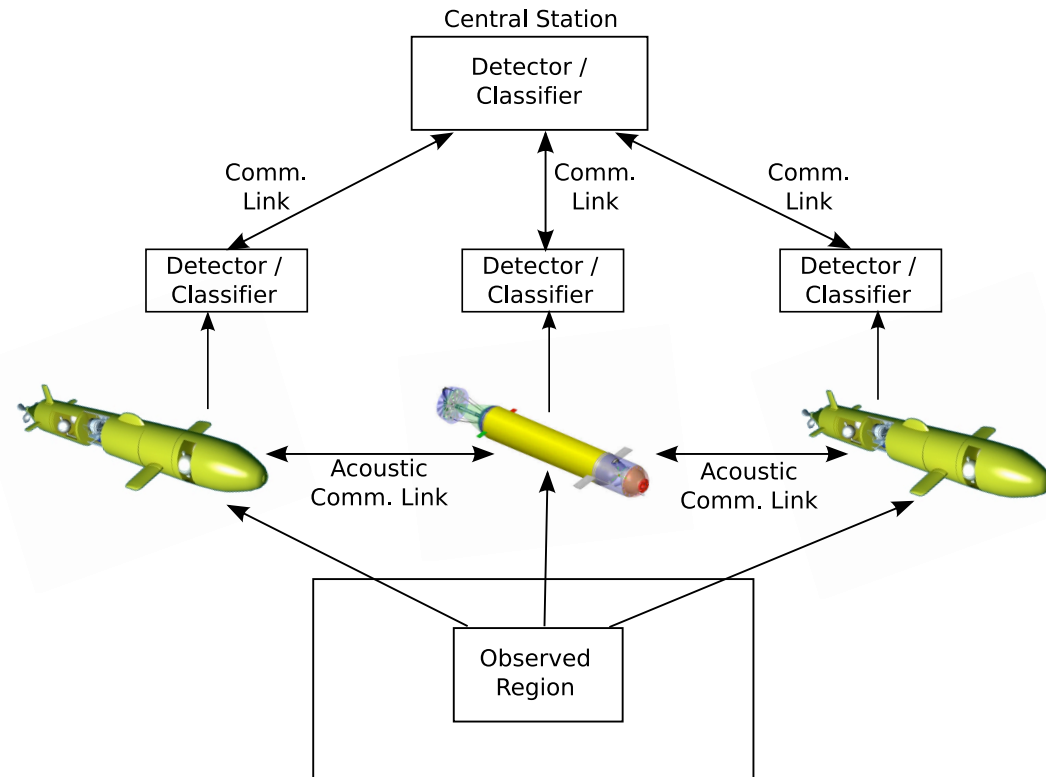


- ✓ Limited Field of View of the Environment
- ✓ Improvement is limited, based on limited data and observations

Distributed Sensor Approach



PMA



NSA

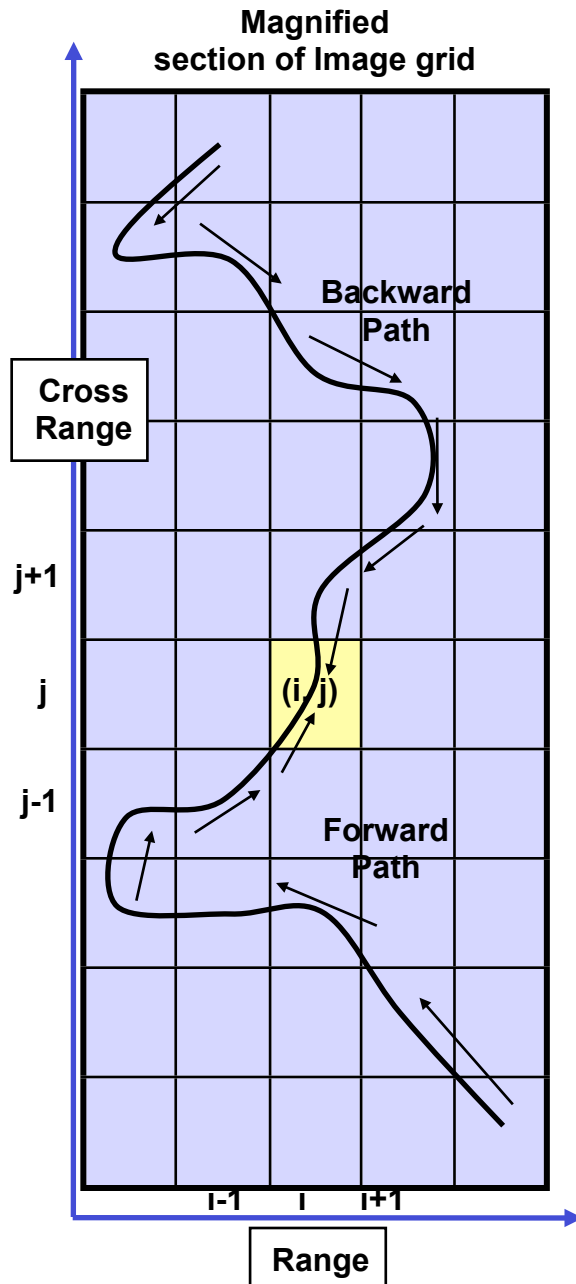
✓ Two Approaches

- Post Mission Analysis (PMA) - all processing done at central station
- Network-centric Sensor Analysis (NSA) - collaboration done among sensors and decision made at sensors

K-Space Beamforming

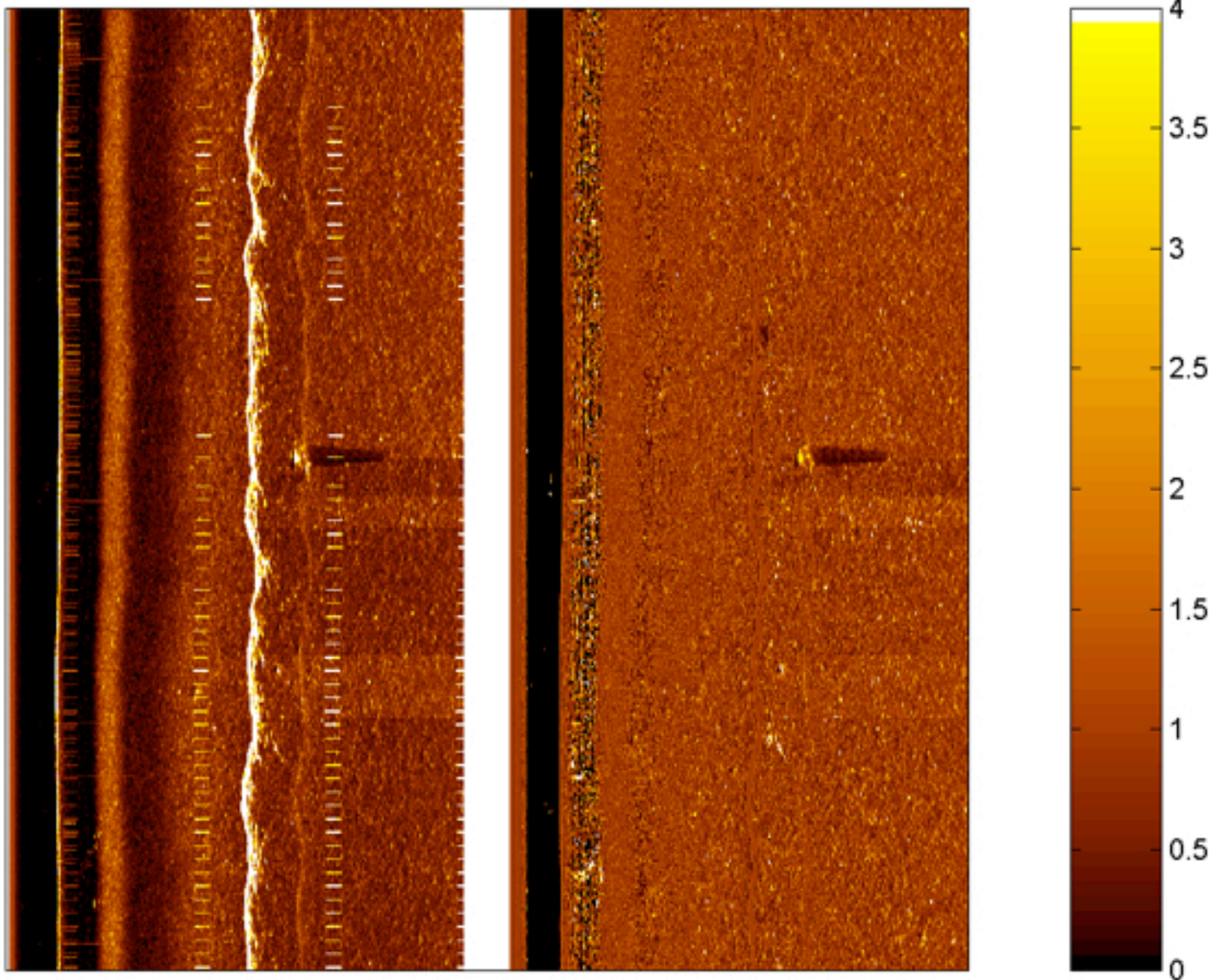
- ✓ Each impinging sound wave on the receiver array elements of the sonar has a magnitude and phase
- ✓ The beamforming algorithm shifts and sums the sound waves using linear shift-invariant signal processing at each element in a way that resolves the echo returns into a pixel of the sonar image. This pixel has a magnitude and phase, and thus is complex.
- ✓ The k-space or wavenumber algorithm computes the 2-D Fourier transform on the raw or range-compressed sonar data where it is in the delay-time/aperture domain.
 - Resolves the data into the temporal frequency/wavenumber (ω, k) domain and then is multiplied by the power spectrum of the transmitted wavefront.
 - Change of variables is done by Stolt interpolation.
 - Maps the (ω, k) domain into the wavenumber domain (k_x, k_y) , where it is the Fourier transform of the image plane.
- ✓ Inverse 2-D Fourier transform of the mapped data to form the complex image.

SFBF Normalizer



- ✓ Attempts to select a path along which the filter output best follows the original image
 - Generated recursively by extending the path's latest end point to one that belongs to a subset of its neighbors whose intensity is most near its filtered output value
- ✓ First, the forward filter proceeds from top-to-bottom.
 - The image is filtered both from left-to-right (L-R) and right-to-left (R-L) to find the pixels that that is nearest the current processed pixel value
- ✓ Second, the backward filter proceeds from bottom-to-top
 - Filtered in both the L-R and R-L directions
- ✓ The pixel (i,j) is normalized the delayed output of either filter that is closes to the pixel's intensity

SFBF Normalization Example



Literature Review

- ✓ (Dobeck SPIE '97) utilized a nonlinear matched filter to identify mine-size regions that match the target template in a side-scan sonar image
 - features were extracted based on the size, shape, and strength of the target template.
 - A k-nearest neighbor and an optimal discrimination filter classifier were used to classify each feature vector. Outputs were fused for final decision
- ✓ (Ciany IEEE Oceans '00) the sonar image is split into overlapping range segments where the pixels in each segment were adaptively thresholded. The threshold was determined from the cumulative histogram formed from a training set. The purpose of the thresholding is to identify the target structure in the processed segments
 - Geometric features were then extracted from the target structure regions
 - Classification of each region as target or non-target was done through a multi-level weighted scoring-based classification system
- ✓ (Aridgides SPIE '08) uses a adaptive clutter filter detector which exploits the difference in correlation characteristics between clutter and targets
 - features were extracted from the detection regions and then orthogonalized by making the eigenvalues of the overall data scatter matrix unity
 - Classification using an optimal Bayesian classifier

CCA-Based Detection

Under H_1 , the composite covariance can be written

$$R_{zz} = E[\mathbf{z}\mathbf{z}^H] = \begin{bmatrix} R_{xx} & R_{xy} \\ R_{yx} & R_{yy} \end{bmatrix} = \begin{bmatrix} R_s & R_s \\ R_s^H & R_1 = R_s + R_0 \end{bmatrix}.$$

The “signal-to-noise ratio” matrix is then $S = R_0^{-1/2}(R_s + R_0)R_0^{-H/2}$

The log-likelihood can then be written as

$$l(\mathbf{y}) = (R_s^{-1/2}\mathbf{y})^H (R_s^{H/2}R_0^{-1}R_s^{1/2} - R_s^{H/2}(R_s + R_0)R_s^{1/2})(R_s^{-1/2}\mathbf{y}).$$

Using the fact $[(CC^H)^{-1} - I]^{-1} = R_s^{H/2}R_0^{-1}R_s^{1/2}$

$$l(\mathbf{y}) = (R_s^{-1/2}\mathbf{y})^H ([(CC^H)^{-1} - I]^{-1} - CC^H)(R_s^{-1/2}\mathbf{y}).$$

Taking the SVD of the coherence matrix $C = R_s^{H/2}R_1^{-H/2} = \mathbf{F}\mathbf{K}\mathbf{G}^H$

$$l(\mathbf{y}) = (\mathbf{G}^H R_1^{-1/2}\mathbf{y})^H ([\mathbf{I} - \mathbf{K}^2]^{-1} - \mathbf{I})(\mathbf{G}^H R_1^{-1/2}\mathbf{y}).$$

or alternatively,

$$l(\mathbf{v}) = \mathbf{v}^H ([\mathbf{I} - \mathbf{K}^2]^{-1} - \mathbf{I})\mathbf{v}$$

Dual Disparate Target Detection

We now have $\bar{Q} = \bar{R}_0^{-1} - \bar{R}_1^{-1}$ with J-divergence $J = tr(-2I + \bar{R}_0^{-1}\bar{R}_1 + \bar{R}_1^{-1}\bar{R}_0)$

$$tr(\bar{R}_0^{-1}\bar{R}_1) = 2tr(R_0^{-1}R_1) = 2tr(S) = 2tr(\Lambda)$$

$$tr(\bar{R}_1^{-1}\bar{R}_0) = \begin{bmatrix} R_1 & R_s \\ R_s & R_1 \end{bmatrix}^{-1} \begin{bmatrix} R_0 & 0 \\ 0 & R_0 \end{bmatrix}$$

Using matrix inversion lemma

$$tr(\bar{R}_1^{-1}\bar{R}_0) = -tr \left(\begin{bmatrix} R_0^{-1}(R_1^{-1} - 2R_0^{-1})^{-1} & R_0^{-1}(R_1^{-1} - 2R_0^{-1})^{-1} + I \\ R_0^{-1}(R_1^{-1} - 2R_0^{-1})^{-1} + I & R_0^{-1}(R_1^{-1} - 2R_0^{-1})^{-1} \end{bmatrix} \right)$$

$$tr(\bar{R}_1^{-1}\bar{R}_0) = -2tr(R_0^{-1}R_1 - R_0^{-1}R_1(I - \frac{1}{2}R_1^{-1}R_0)^{-1}) = -2tr(S - S(I - \frac{1}{2}S^{-1})^{-1})$$

J - divergence is now

$$J = tr(-2I + 2\Lambda(I - \frac{1}{2}\Lambda^{-1})^{-1}) = \sum_{i=1}^n -2 + \frac{4\lambda_i^2}{2\lambda_i - 1}.$$

using the relationship $\lambda_i = \frac{1}{1 - k_i^2}$, $J = \sum_{i=1}^n -2 + \frac{4}{1 - k_i^4}.$

Dual Disparate Target Detection

We can now rewrite \bar{Q} and express the log-likelihood as

$$l(\mathbf{z}) = \mathbf{z}^H \begin{bmatrix} R_0^{-1} + R_0^{-1}(R_1^{-1} - 2R_0^{-1})^{-1}R_0^{-1} & R_0^{-1} + R_0^{-1}(R_1^{-1} - 2R_0^{-1})^{-1}R_0^{-1} \\ R_0^{-1} + R_0^{-1}(R_1^{-1} - 2R_0^{-1})^{-1}R_0^{-1} & R_0^{-1} + R_0^{-1}(R_1^{-1} - 2R_0^{-1})^{-1}R_0^{-1} \end{bmatrix} \mathbf{z}.$$

Using matrix inversion lemma

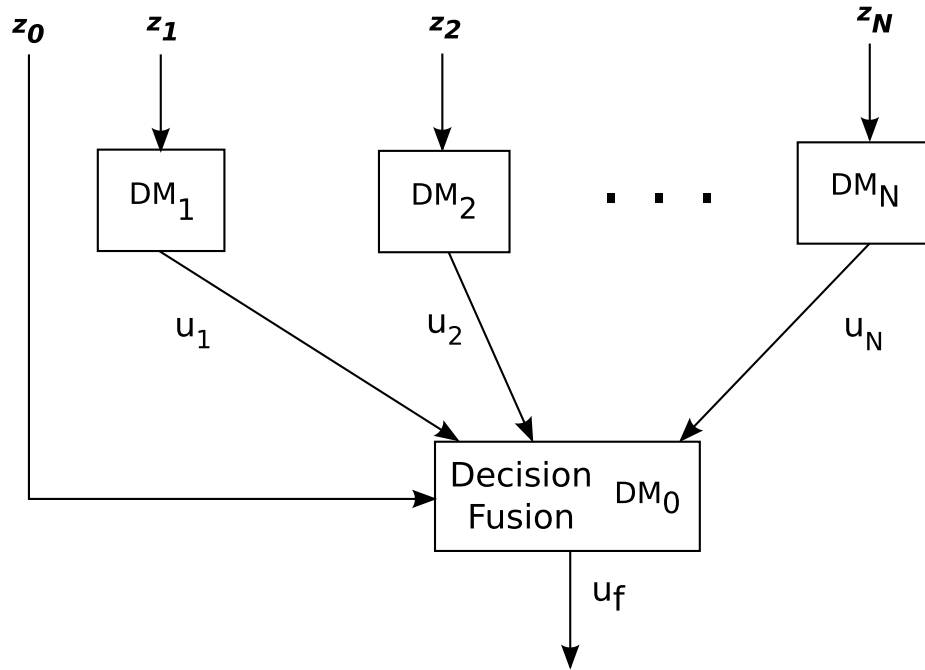
$$l(\boldsymbol{\eta}) = \boldsymbol{\eta}^H \begin{bmatrix} \mathbf{I} + (\mathbf{S}^{-1} - 2\mathbf{I})^{-1} & \mathbf{I} + (\mathbf{S}^{-1} - 2\mathbf{I})^{-1} \\ \mathbf{I} + (\mathbf{S}^{-1} - 2\mathbf{I})^{-1} & \mathbf{I} + (\mathbf{S}^{-1} - 2\mathbf{I})^{-1} \end{bmatrix} \boldsymbol{\eta}. \text{ where } \boldsymbol{\eta} = \begin{bmatrix} R_0^{-1/2} & 0 \\ 0 & R_0^{-1/2} \end{bmatrix} \mathbf{z}$$

Expressing in terms of the SVD of the coherence matrix $\mathbf{C} = R_0^{H/2} R_1^{-H/2} = \mathbf{F}\mathbf{K}\mathbf{G}^H$

and using the fact $\mathbf{F}^H R_0^{-1/2} = \mathbf{K}^{-1}\mathbf{G}^H R_1^{-1/2}$

$$l(\mathbf{w}) = \mathbf{w}^H \begin{bmatrix} 1/2\mathbf{I} - 1/4(\mathbf{K}^{-2} - 1/2\mathbf{I})^{-1} & 1/2\mathbf{K}^{-1} - 1/4(\mathbf{K}^{-1} - 1/2\mathbf{K})^{-1} \\ 1/2\mathbf{K}^{-1} - 1/4(\mathbf{K}^{-1} - 1/2\mathbf{K})^{-1} & 1/2\mathbf{K}^{-2} - 1/4(\mathbf{I} - 1/2\mathbf{K}^2)^{-1} \end{bmatrix} \mathbf{w}$$

Distributed Detection



If the local decision makers rules are known the optimum fusion is a rule is a likelihood-ratio as it is just a centralized detection problems

Using Bayes' rule we can rewrite the fusion rule as

$$\gamma_f(u_1, \dots, u_N, \mathbf{z}_0) = \frac{p(H_1|\mathbf{z}_0)}{p(H_0|\mathbf{z}_0)} \frac{\prod_{i=1}^N p(H_1|u_i)}{\prod_{i=1}^N p(H_0|u_i)} \underset{H_0}{\overset{H_1}{\gtrless}} \frac{P_1^N [C_{10} - C_{00}]}{P_0^N [C_{01} - C_{11}]}$$

Sample Poor Gauss-Gauss Detection

Taking the SVD of the data matrices

$$\begin{aligned} X &= V_1 \Lambda_X V_2^H \\ Y &= W_1 \Lambda_Y W_2^H \end{aligned} \quad \Lambda_X = \begin{bmatrix} \Lambda_X(p) & \mathbf{0} \\ \mathbf{0} & \mathbf{0} \end{bmatrix}, \Lambda_Y = \begin{bmatrix} \Lambda_Y(p) & \mathbf{0} \\ \mathbf{0} & \mathbf{0} \end{bmatrix}$$

The “signal-to-noise ratio” matrix is of rank p

$$\begin{aligned} \hat{S}_p &= (V_{1,p} \Lambda_X^2(p) V_{1,p}^H)^{-1/2} (W_{1,p} \Lambda_Y^2(p) W_{2,p}^H) (V_{1,p} \Lambda_X^2(p) V_{1,p}^H)^{-H/2} \\ &= U_p \Lambda(p) U_p^H \end{aligned}$$

Define $D_p \triangleq (X X^H)^{-H/2} U_p$

$$(Y Y^H) D_p = (X X^H) D_p \Lambda(p).$$

Since D_p is in the span of X , we can write $D_p = X A_p$, therefore

$$(X^H Y)(Y^H X) A_p = (X^H X)(X^H X) A_p \Lambda(p),$$

and the log-likelihood can be expressed as,

$$l(\mathbf{x}) = \mathbf{x}^H X (\mathbf{I} - A_p \Lambda^{-1}(p) A_p^H) X^H \mathbf{x}.$$

Eigenvalue Gap and SNR

Let γ_1 and γ_{12} be the largest and smallest eigenvalues of R_s

The eigenvalue gap is then

$$(\lambda_1/\lambda_{12}) = (\gamma_1 + \sigma_n^2)/(\gamma_{12} + \sigma_n^2) \approx (SNR + 1)/(\gamma_{12}/\sigma_n^2 + 1)$$

It is assumed that $R_0 = \sigma_n^2 I$, since the eigenvalues are fixed as $SNR \approx \gamma_1/\sigma_n^2$, decreases, the gap will increase.

